

# Fabrication of textured alumina by orienting template particles during electrophoretic deposition

Li Zhang\*, Jef Vleugels, Omer Van der Biest

*K.U.Leuven, Department of Metallurgy and Materials Engineering, Kasteelpark Arenberg 44, B-3001 Heverlee, Belgium*

Available online 16 July 2009

## Abstract

(001)-Textured  $\alpha$ -alumina has been processed by electrophoretic deposition (EPD) and templated grain growth. The mechanism of platelet template orientation during EPD was examined with respect to the impact of the electric field force, gravity and hydrodynamic force in two different deposition cells with vertically or horizontally positioned deposition electrodes. A sharp (001) ‘fibre texture’ was obtained after templated grain growth during sintering of a deposit formed from a stirred 5 vol% platelet containing suspension in a vertical deposition cell. The texture was characterized by means of the Lotgering factor, texture index and electron backscattering diffraction (EBSD).

© 2009 Elsevier Ltd. All rights reserved.

**Keywords:** Suspensions; Platelets;  $\text{Al}_2\text{O}_3$ ; Texture

## 1. Introduction

Textured materials have been investigated extensively in the past few years due to their improved electronic and structural properties. If polycrystalline particles could be aligned, they may be able to exhibit the anisotropic characteristics typical of single crystals.<sup>1</sup> For instance, as an important engineering ceramic, textured  $\alpha$ -alumina is widely investigated and the property of this textured  $\alpha$ -alumina was reported to be significantly enhanced.<sup>2–4</sup> Textured materials can be produced by a variety of techniques including magnetic orientation and templated grain growth (TGG).<sup>3–6</sup> Templated grain growth is widely investigated.<sup>4–6</sup> Large and anisotropically shaped template particles are homogeneously aligned in a fine matrix powder during compacting. During sintering, textured material was obtained by grain growth in the anisotropic direction of the aligned template particles. The template alignment in the green compact is a critical factor in TGG since it determines the final texturisation. Templates could be aligned by various powder consolidation techniques including uniaxial pressing, slip casting, tape casting, gel casting, centrifugal casting and extrusion.<sup>5–9</sup> In those cases, the active forces orientate the template grains during the powder consolidation process.

This work shows the possibility to align platelet template during electrophoretic deposition (EPD). EPD is a colloidal process wherein particles suspended in a stable suspension are deposited on one of the electrodes by applying an electric field. The simplicity in experimental set-up leads to low equipment cost. EPD is also a fast compacting technique and the deposit thickness can be easily controlled. EPD has the capability to form complex shapes and patterns. Moreover, EPD can be applied on a wide range of substrates such as porous ceramics, conductive polymers or metals.<sup>10,11</sup>

In this study, hexagonal  $\alpha$ -alumina platelet templates were aligned in a fine matrix alumina powder by EPD. After templated grain growth, a highly textured material was developed. The mechanism of platelet alignment during deposition was investigated considering the impact of orientation forces.

## 2. Experimental procedure

High purity fine  $\alpha$ -alumina powder ( $\sim 0.3 \mu\text{m}$ , Baikowski grade SM8, France) was used as matrix powder, whilst hexagonal alumina platelets ( $10\text{--}15 \mu\text{m}$  in diameter,  $\sim 0.5 \mu\text{m}$  thick, ELF Atochem, France) were used as templates. The morphology of the alumina matrix powder and platelet template is shown in Fig. 1. Fine alumina matrix powder suspensions were initially milled for 24 h on a multi-directional mixer (type Turbula, WAB, Switzerland) at 70 rpm in absolute ethanol (99.9% Merck Belgium) with 0.5 vol% de-ionised water. Zirconia milling balls

\* Corresponding author. Tel.: +32 16 321777; fax: +32 16 321992.  
E-mail address: [Li.Zhang@mtm.kuleuven.be](mailto:Li.Zhang@mtm.kuleuven.be) (L. Zhang).

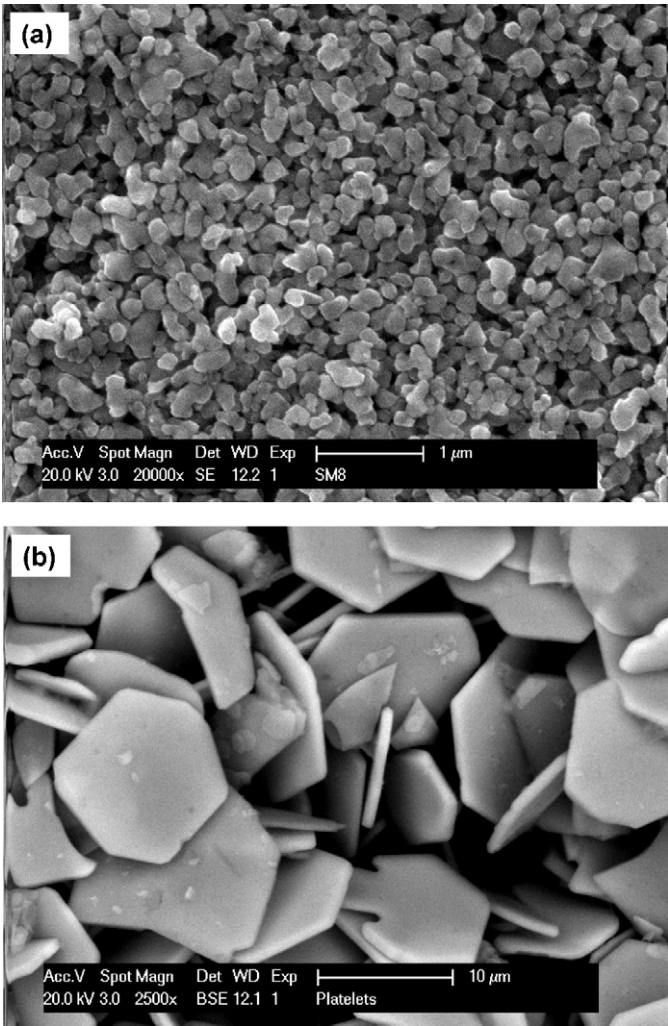


Fig. 1. SEM image of (a) as-received alumina grade SM8 and (b) platelets.

(Tosoh grade TZ-3Y) with a diameter of 5 mm were added to the polyethylene container to facilitate breaking the agglomerates. Afterwards, platelets (5 wt% relative to the total amount of powder) were added to the ball-milled suspension, whilst *n*-butylamine (99.5% Acros Belgium, 3.4 vol% relative to the suspension volume) was added to negatively charge the particles and Dolapix Ce-64 (Zschimmer & Schwarz, Germany, 1.1 wt% relative to the powder mass) was added as dispersant. For comparison, a suspension without platelets was also prepared. This suspension was magnetically stirred for 60 min, ultrasonicated in an ultrasonic bath (Branson 2510) for 15 min and magnetically stirred for another 15 min.

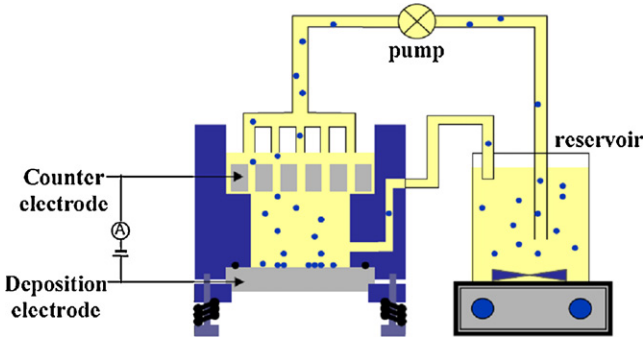


Fig. 2. EPD cell with horizontally positioned deposition electrode.

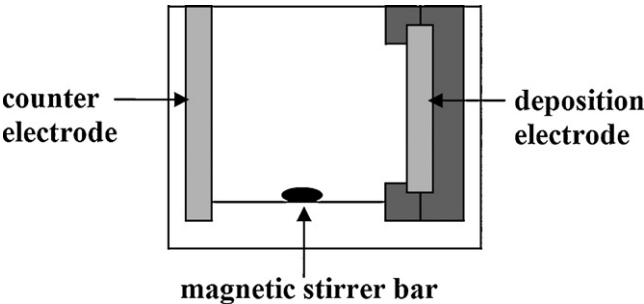


Fig. 3. EPD cell with vertically positioned deposition electrode.

To estimate the influence of the electric field force, gravity and hydrodynamic force on the alignment of the platelets, two different set-ups were used, i.e., with a vertical and horizontal EPD cell. Three configurations were studied in a slightly modified horizontal cell, as summarised in Table 1. The standard horizontal EPD cell is schematically presented in Fig. 2. In case of an applied suspension flow (configuration 2 in Table 1), a suspension was flown through the deposition cell by means of a suspension circulation system driven by a peristaltic pump. The distance between the flat disc shaped electrodes was 3.5 cm and the electrodes had a diameter of 3.7 cm. The suspension in the reservoir was stirred to avoid sedimentation. In addition, the flow-through system also decreases the sedimentation of the suspension in the cell with the fluid flow. Homogeneous deposits were made by pumping 200 ml suspension at 1 ml/s through the deposition cell. The suspension circulation system was not used in the other two configurations (3 and 4 of Table 1) where only 50 ml suspension was used to fill the EPD cell. Configuration 4 and 3 form respectively depositions along and in the opposite direction of the gravity force, in which the perforated top electrode (Fig. 2) was replaced with a normal one. EPD was con-

Table 1  
Density, Lotgering factor and texture index for different EPD configurations.

Configuration	Cell	Deposition	Suspension	Green density [%]	Sintered density [%]	Lotgering factor	Texture index
1	Vertical	Vertical	stirred	59.4	97.9	0.49	18.32
2	Horizontal	Bottom	Flow through	58.9	97.5	0.01	1.60
3	Horizontal	Top	Stagnant	62.7	99.7	0.21	8.12
4	Horizontal	Bottom	Stagnant	61.1	98.0	0.02	2.52
5	Vertical	Vertical	Stagnant	–	–	0.12	8.05

ducted for 450 s. The 50 ml vertical EPD cell, presented in Fig. 3, consisted of two vertically positioned electrodes with a separation distance of 3.5 cm and a surface area of 9 cm<sup>2</sup>. The edges of the deposition electrode were shielded by a non-conductive PTFE cover. Two configurations were studied in the vertical cell, i.e., with a stagnant (configuration 5) and a magnetically stirred (~250 rpm) (configuration 1) suspension.

Constant voltage anodic electrophoretic deposition was performed with freshly prepared suspensions, using a F.U.G. (type MCN 1400-50) power supply. The pH\* of the suspension before EPD was 11.45. pH\* denotes the operational pH for which a standard pH electrode was used to measure the pH in ethanol suspensions.<sup>12</sup> The conductivity of the suspension at room temperature was 24.5  $\mu$ S/cm, as measured by a conductivity sensor (Cond Level 2 type, WTW). After EPD, the deposit was carefully removed from the suspension and dried in air. Afterwards, the deposit was sintered in air (Nabertherm furnace, Germany) at 1550 °C for 1 h with a heating rate of 10 °C/min. The green and sintered density was measured in ethanol by the Archimedes method.

The microstructure of the polished and thermally etched surface of sintered samples was investigated by scanning electron microscopy (SEM, XL30-FEG, FEI, Netherlands). Texture analysis was performed by X-ray diffraction (type Seifert 3003), pole figure measurements (Siemens D500 Texture & Stress) and Electron Back-Scatter Diffraction (EBSD, EDAX, Netherlands).

The Lotgering factor is widely used in literature to characterize the texture degree of hexagonal  $\alpha$ -alumina,<sup>13,14</sup> and can be obtained from the X-ray diffraction pattern of a sample. The Lotgering factor is defined as:

$$f = \frac{(\sum I(00l) / \sum I(hkl)) - (\sum I^0(00l) / \sum I^0(hkl))}{1 - (\sum I^0(00l) / \sum I^0(hkl))} \quad (1)$$

with  $\sum I(00l)$ , the summation of all (00 $l$ ) peak intensities and  $\sum I(hkl)$ , the summation of all peak intensities in the spectrum. Superscript 0 corresponds to a random sample. The  $f$  factor changes between 0 and 1. A large  $f$  value implies a highly textured material, since  $f=0$  for a random sample and  $f=1$  for a fully oriented material.

In order to give a complete estimation of texture formation, the texture index was calculated depending on the orientation distribution function (ODF). The ODF was obtained from measured pole figures by “Hexagonal ODF software system” (Dept MTM—K.U.Leuven). The texture index was used as an indicator of the sharpness of the texture, and is defined as the integral of the square of the ODF,  $f(g)$ , over the entire orientation space<sup>15</sup>:

$$\text{T.I.} = \oint [f(g)]^2 dg \quad (2)$$

The higher the value, the sharper the texture. A value close to 1 implies random texture.

EBSD was used to examine the microstructure and the regional grain orientation. The examined area was 180  $\times$  520  $\mu$ m<sup>2</sup> and the step size was 1  $\mu$ m. The grain orientation maps and inverse pole figures were all generated from the experimental data using commercial software (TSL OIM analysis 4.5).

### 3. Results

#### 3.1. Vertical deposition from a stirred suspension

The influence of the platelet template can be assessed by comparison with the random alumina powder based ceramic. The texture of the platelets containing material was confirmed by XRD, as shown in Fig. 4. The diffraction spectrum of the random ceramic (Fig. 4(a)) is consistent with the JCPDS card of alumina (card number 43-1484), which means that no significant texture was formed in the sample. The (1 1 0) and (3 0 0) diffraction peak intensities are pronounced in the spectrum of the sample, cross-sectioned perpendicular to the deposition electrode (perpendicular section, see Fig. 4(b)). Those peaks are stronger than in the random sample as well as in the sample cross-sectioned parallel to the electrode (parallel section, see Fig. 4(c)). The (0 0 6) and (0 0 12) peaks are hardly observed in the perpendicular section and the random sample, whereas they are prominent in the parallel section. The (1 0 4) and (1 0 10) peaks are also stronger in the parallel section than in the random sample and the perpendicular section. These results imply that a large volume fraction of strong (0 0 1) textured alumina grains are formed in the platelet containing material. The  $c$ -axis is oriented perpendicular to the surface of the deposition electrode. Based on the XRD spectrum, the Lotgering factor is calculated to be 0.49, which implies a well-textured material.

The microstructural anisotropy is confirmed by the SEM micrographs shown in Fig. 5. SEM analysis at different locations in the sintered deposit revealed that the platelet particles are nearly homogeneously distributed throughout the deposits. The seeded platelets acted as templates for the grain growth during sintering. The basal planes of the grown platelets have been aligned parallel to the surface of the deposition electrode. During sintering, the aligned platelet seeds grew very fast by means of coarsening, i.e., by the consumption of the fine matrix alumina particles, resulting in a highly textured ceramic. Grain growth has been fast by means of grain boundary migration since there is a substantial amount of pores trapped inside the grains. Intergranular pores are also clearly observed in Fig. 5. The relative density of this ceramic is 97.9%. Beside the intergranular

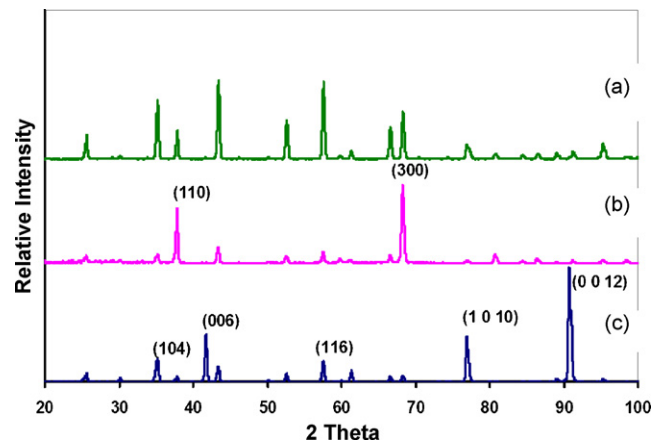


Fig. 4. X-ray diffraction pattern of sintered (a) a random alumina sample and cross-sectioned template containing ceramic (b) perpendicular and (c) parallel to the electrode surface.



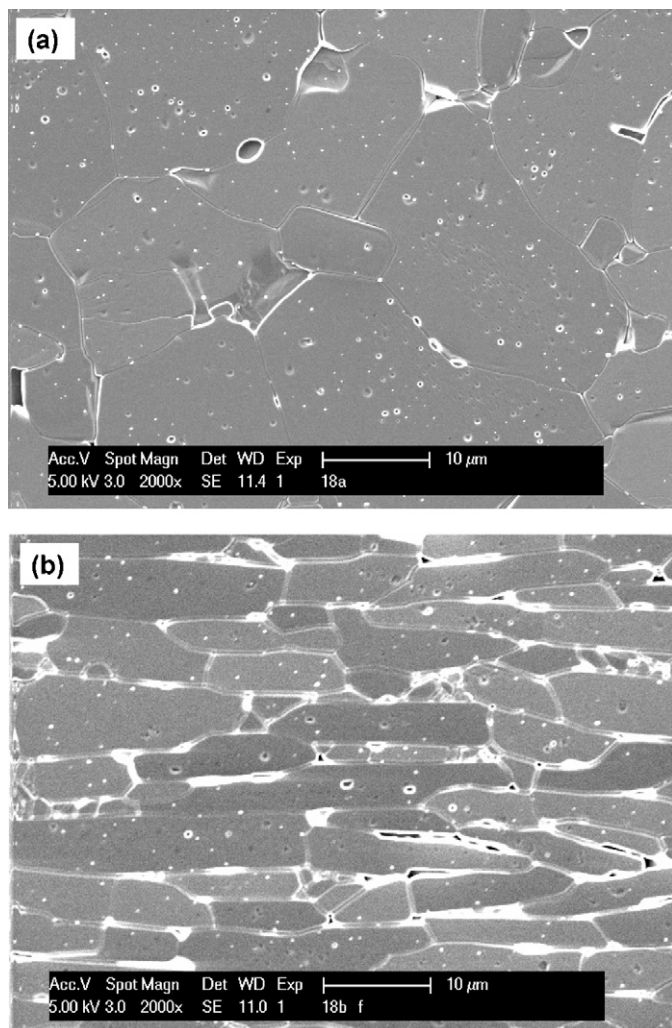


Fig. 5. Textured alumina deposited in a horizontal cell, cross-sectioned (a) parallel and (b) perpendicular to the deposition electrode.

porosity, the residual porosity also results from platelet particle constrained sintering, as discussed in literature.<sup>16,17</sup> Since the template platelets are essential for texture development, all further investigated grades were prepared from platelet containing suspensions.

EBSD of perpendicularly cross-sectioned grades was investigated to characterize the texture. The EBSD pattern and inverse pole figure (IPF) of the above material grade are presented in Fig. 6(a) and (d). The platelets are well aligned parallel to the deposition electrode surface, positioned at the bottom of the picture in Fig. 6(a), revealing that the *c*-axis has been well-aligned perpendicular to the surface of the deposition electrode, as shown in Fig. 6(a). The peak intensity of the [0 0 1] IPF shown in Fig. 6(d) is large and the peak is homogeneously distributed at the edge of the IPF, proving that the prismatic planes are well oriented in the normal direction. The *a*- and *b*-axes are not aligned, i.e., the material has no preferred in-plane orientation (*a*-axis or *b*-axis orientation) as indicated by the fact that the peak intensity is homogeneously distributed at the edge of the IPF.

In order to investigate the global sample area, X-ray pole figures were used to characterize the macro-texture. The calcu-

lated texture index of this sample is 18.32, which implies a sharp texture formation.

### 3.2. Horizontal downward deposition from a flowing suspension

The same suspension composition was used for EPD in the horizontal cell, shown in Fig. 2, with the deposition electrode at the bottom and suspension flowing through. The platelets in the deposit however were not well aligned as shown in the EBSD pattern of the perpendicular cross-section of the sintered ceramic (Fig. 6(b)). As shown in Fig. 6(e), the peaks are relatively weak and are not homogeneously distributed implying that the prismatic planes are not well aligned. The corresponding X-ray pole figure confirms a very weak texturing after grain growth with a limited texture index of 1.60.

### 3.3. Deposition from a stagnant suspension

The above results clearly show that the cell geometry is a critical factor for platelet alignment during EPD. The electric field force, gravity and hydrodynamic force applied on the platelets are believed to be the main factors influencing platelet alignment. The influence of these forces is studied using 3 additional configurations as summarised in Table 1. In order to investigate the electric field force effect, an upward deposition was performed in the horizontal cell without suspension flowing through (configuration 3). In order to investigate the gravity effect, EPD was performed from a stagnant suspension in the horizontal cell (configuration 4). In order to study the impact of the hydrodynamic force, the suspension is stirred comparing with stagnant suspension (configuration 5) or pumped through the cell as described in Sections 3.1 and 3.2.

Table 1 summarises the Lotgering factor and texture index measured on the parallel cross-sectioned sintered deposits obtained under different EPD cell configurations, as well as the green and sintered density. The green relative density of all the deposits was in the 58.9–62.7% range, which is quite comparable. After sintering, quite dense ceramics with some remaining porosity due to constrained sintering were obtained. The densification of the powder matrix is significantly retarded by the presence of large inclusions, i.e., platelets, resulting in a lower densification as reported in literature.<sup>16,17</sup> The sintered density is proportional to the green density of the samples, as shown in Table 1. EPD from a stirred suspension in a vertical cell (configuration 1) results in the highest Lotgering factor and texture index, which indicates that the best texture was formed. The extent of texturisation is quite different for the five investigated configurations. The mechanism of texture formation is discussed below, based on these experimental findings.

## 4. Discussion

### 4.1. Influence of the electric field force

The electric field force is the driving force for powder consolidation during EPD. In order to investigate the impact of the electric field force on platelet alignment, EPD from a stagnant



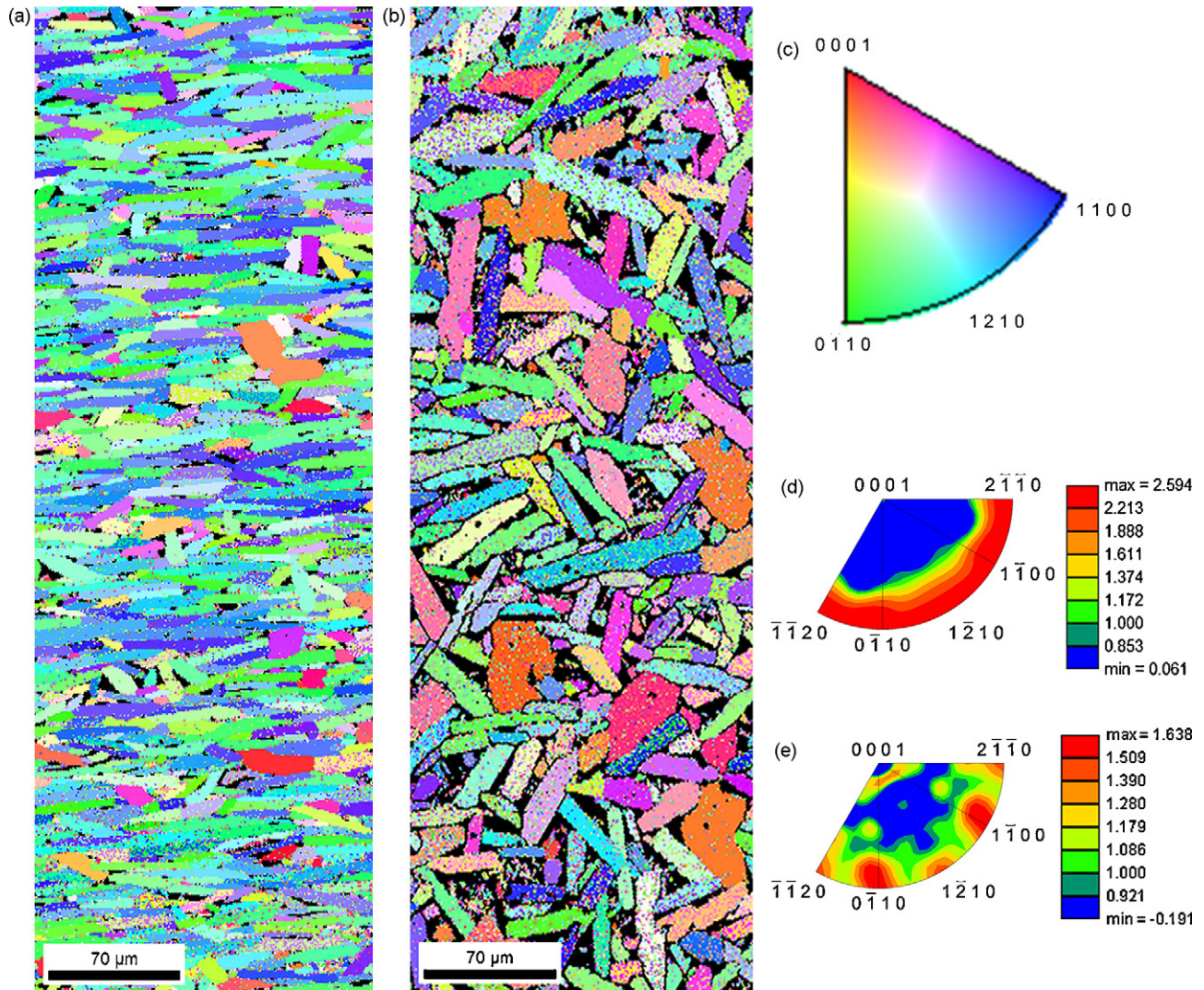


Fig. 6. EBSD data on a textured alumina. EBSD pattern of the perpendicular cross-section of the sample formed (a) in vertical cell with stirred suspension; (b) in horizontal cell with suspension flowing through; (c) corresponding colour coded map and (d) [00 1] IPF for (a), and (e) [00 1] IPF for (b).

suspension in a horizontal cell with a deposition electrode on the top (configuration 3) was investigated. In this case, the downward gravity force on the platelets is counteracted by the upward electric field force and the platelet alignment in the deposit is mainly induced by the electric field force. As shown in Fig. 7, the basal planes of the platelets are well aligned parallel to the deposition electrode surface. The electric field force can orientate the platelets in two possible ways, i.e., during electrophoresis or upon deposition.

One possible mechanism is that the electric field force aligns the platelets during electrophoresis due to the charge distribution on the platelet surfaces. The electrical charge on the basal plane of the platelets is different from that on the side plane due to the large difference in surface area. Under the present experimental conditions at pH 11.4, all platelet surfaces are negatively charged although the natural charge density could be different between the basal plane and prismatic plane.<sup>18–20</sup> The electric field force applied on the basal plane is therefore larger than on the prismatic plane. The platelet alignment mechanism may depend on the polarisation of the electrical double layer in the electric field,

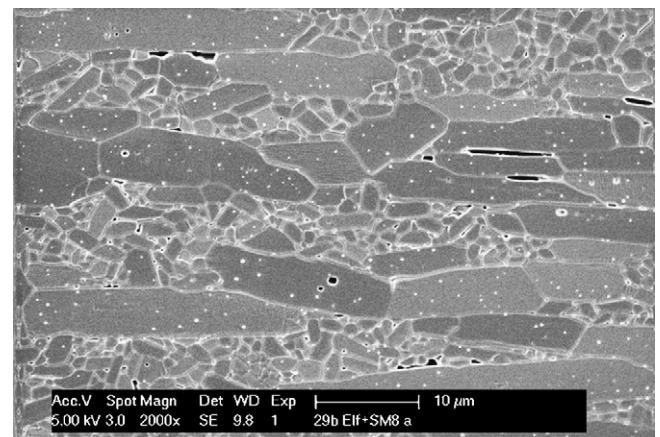


Fig. 7. SEM micrograph of a perpendicularly cross-sectioned ceramic obtained by upward EPD in a horizontal cell without suspension flowing through.



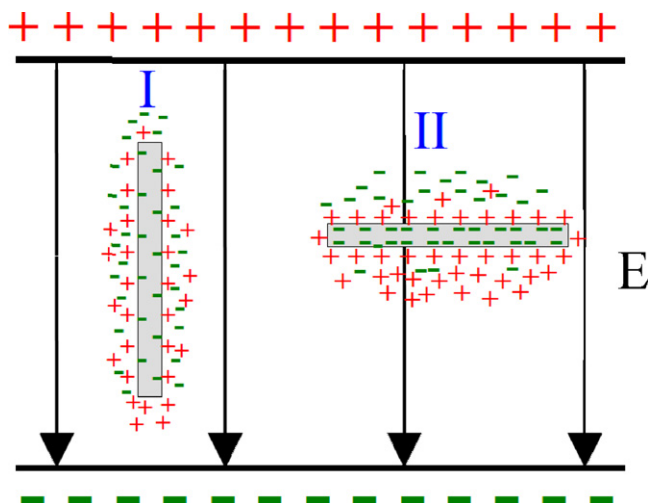


Fig. 8. Schematic illustration of the platelet orientation in an applied electric field during EPD.

mainly from the basal plane. This might be explained by the difference in charge density on platelets oriented parallel or perpendicular to the electric field. The negatively charged alumina platelets gather a diffuse double layer of counter ions around them, which becomes asymmetrically polarised in the electric field. If the platelet is initially oriented parallel to the electric field (case I in Fig. 8), the positive ions above the basal plane in-between the platelet and the anode will try to counteract the electrical force on the platelet, resulting in a reduced platelet mobility in the electric field. However, if the platelet is initially positioned parallel with respect to the electrodes (case II in Fig. 8), polarisation of the diffuse ion cloud is easier resulting in preferred deposition. This would actually imply that the platelets are oriented perpendicularly to the electric field during electrophoresis. It should also be noted that when particles are moving towards the electrode during EPD, there is a hydrodynamic force in the opposite direction due to the fact that the solvent has to move in the opposite direction of particle movement. That could also influence the alignment of platelets. Mody et al. observed flipping over of platelets in a parallel-plate flow cell.<sup>21</sup> Under the impact of the hydrodynamic force during electrophoresis, the platelets may also move in a rotational flip-over way.

Another mechanism for platelet alignment might be attributed to the reorientation of platelets once they make contact with the deposit or the deposition electrode. As modelled by Harnau et al., based on density functional theory plate-like particles in the vicinity of a hard wall will adopt nearly a fully parallel alignment due to interactions with the wall.<sup>22</sup> When applying this model to the electrode surface during EPD, the platelet templates will align parallel to the deposition electrode irrespective of their orientation in the suspension. However, the surface charge influence is ignored in this model.

#### 4.2. Influence of gravity

The effect of gravity on platelet orientation during sedimentation depends on many parameters. As reported in literature,

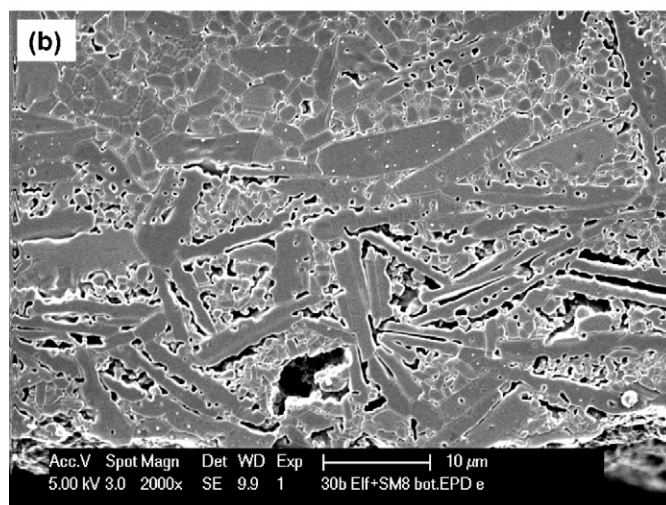
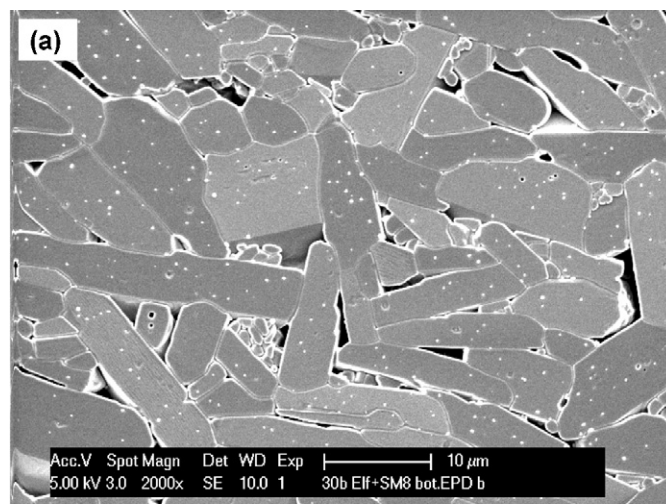


Fig. 9. SEM micrograph of the ceramic obtained (a) after downward deposition in a horizontal cell without suspension flowing through and (b) detail of the electrode contact side revealing sedimentation prior to EPD.

anisotropic platelets can be orientated with their basal plane perpendicular to the gravity direction in the sediment although their basal plane could be parallel to the gravity direction during sedimentation in the suspensions.<sup>23,24</sup>

When depositing in the opposite direction of the gravity force (configuration 3 in Table 1), the platelets were found to be oriented with their basal plane parallel to the surface of the deposition electrode, as discussed above. When depositing along the direction of the gravity force (configuration 4 in Table 1), the platelets were not aligned, as shown in Fig. 9(a). This could be attributed to the interference of platelet sedimentation. Gravity causes the sedimentation of larger particles, especially platelets, due to their relatively larger mass. Prior to EPD, i.e., before applying the voltage, suspension sedimentation was already initiated, as shown in Fig. 9(b). It should also be noted that a downward electric field force speeds up powder settling. The platelet orientation in the deposit is quite weak when EPD along the gravity force, as indicated by the Lotgering factor of 0.02 and texture index of 2.52 in Table 1, whereas texturing is more pronounced when depositing in the opposite direction of gravity.

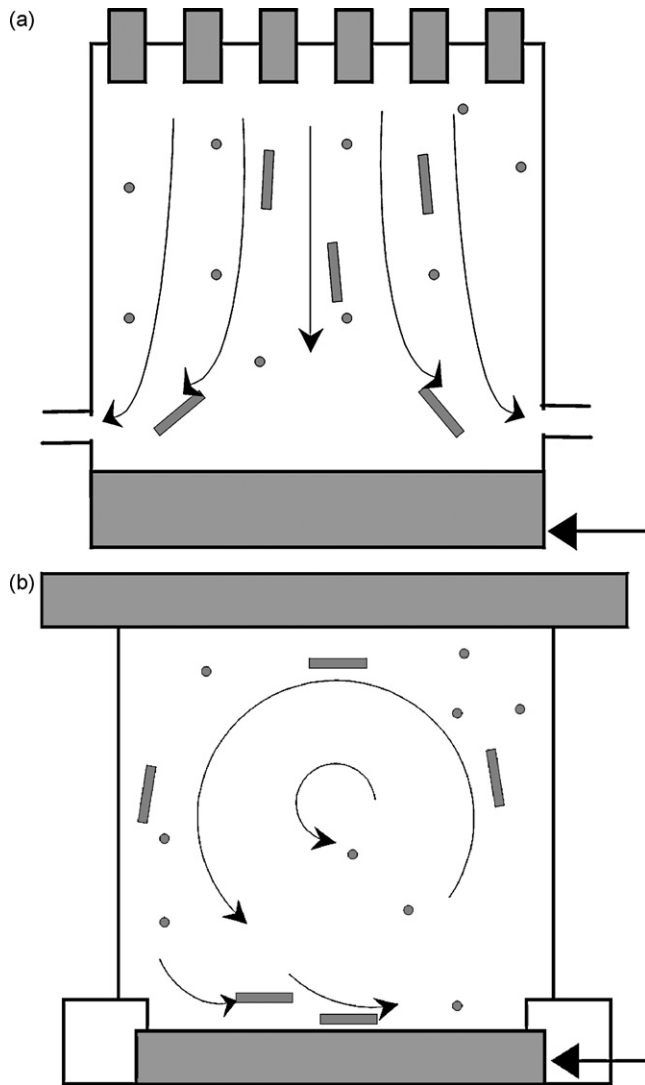


Fig. 10. Flow pattern during EPD (a) in a cross-sectioned horizontal cell with suspension flowing through and (b) top view of the flow pattern during EPD in a vertical cell with magnetic stirring. The deposition electrode is marked by the arrow at the bottom.

#### 4.3. Influence of the hydrodynamic force

When stirring the suspension or generating a suspension flow in the EPD cell, the generated hydrodynamic force in the neighbourhood of the deposition electrode will influence the deposition process. The hydrodynamic force in the horizontal cell is different than in the vertical cell, as schematically presented in Fig. 10. The basal plane of the platelets would be aligned along the fluid direction in order to minimize the dragging force. As shown in Fig. 10(a), the hydrodynamic force is not parallel to the electrode surface in the horizontal cell, which may interfere with the alignment of the platelets. The platelets are indeed not well aligned as shown in Fig. 6(b). In the vertical cell, however, the shear force applied by the fluid flow is almost parallel to the electrode surface, as illustrated in Fig. 10(b). In this case, the hydrodynamic force assists in aligning the basal plane of the platelets parallel to the deposition electrode sur-

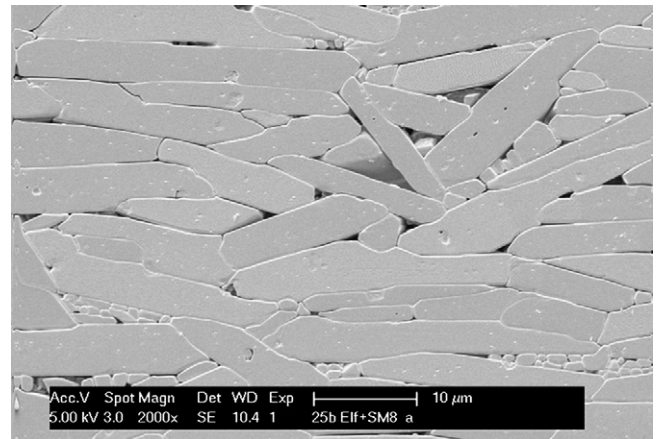


Fig. 11. SEM micrograph revealing the microstructure of a perpendicularly cross-sectioned sintered ceramic after EPD from a stagnant suspension in a vertical cell.

face. Platelet alignment is substantially better when stirring the suspension (Fig. 5 (b)) than without stirring (Fig. 11). Moreover, stirring completely inhibited suspension sedimentation. As a result, the magnetically stirred vertical EPD cell (configuration 1) gives the best texture, as shown in Table 1. It should also be noted that the magnitude of the hydrodynamic force in the two EPD cells is different. The suspension flows through the horizontal cell with a volume of about 50 ml at 1 ml/s. In the vertical cell, the magnetic stirrer stirred 50 ml of suspension at ~250 rpm. The hydrodynamic force is therefore substantially lower in the horizontal cell. The influence of a fluid flow on platelet orientation in the horizontal cell is limited, as shown by the comparable Lotgering factors (0.01 versus 0.02) and texture indexes (1.60 versus 2.52) in Table 1. In the vertical cell, the shear force applied by the fluid is an important factor for platelet orientation, as indicated by the significant increase in Lotgering factor from 0.12 to 0.49 and texture index from 8.05 to 18.32, as induced by the hydrodynamic force.

## 5. Conclusions

Platelet template particles used for templated grain growth could be aligned during the electrophoretic deposition process. The influence of the electric field force, gravity and hydrodynamic force are studied in a vertical and horizontal deposition cell. The electric field force orients the *c*-axis of the platelets parallel to the electric field force direction. Powder sedimentation induced by gravity however is detrimental for platelet alignment in the deposit. The hydrodynamic force aligns the basal plane parallel to the suspension flow direction. The ceramics processed under different EPD configurations result in a different degree of texture, implying that the EPD deposition cell configuration is a critical factor for the platelet template alignment. The highest (001) alumina texture, with a Lotgering factor of 0.49 and texture index of 18.32, was obtained after templated grain growth of the deposits obtained from a vertical EPD cell configuration with a stirred suspension.

## Acknowledgements

This work was performed within the framework of the Research Fund of K.U.Leuven under project GOA/2005/08/TBA and GOA/2008/007. The authors also acknowledge the support of the Flemish Institute for the Promotion of Scientific Technological Research in Industry (IWT) under contract SBO-PROMAG (60056).

## References

1. Randle, V. and Engler, O., *Introduction to texture analysis*. Gordon and Breach Science Publishers, 2000, pp. 3–11.
2. Zhou, Y., Vleugels, J., Laoui, T. and Van der Biest, O., Toughening of X-Sialon with  $\text{Al}_2\text{O}_3$  Platelets. *J Eur Ceram Soc*, 1995, **15**, 297–305.
3. Uchikoshi, T., Suzuki, T. S. and Sakka, Y., Crystalline orientation of alumina ceramics prepared by electrophoretic deposition under a high magnetic field. *J Mater Sci*, 2006, **41**, 8074–8078.
4. Carisey, T., Levin, I. and Brandon, D. G., Microstructure and mechanical properties of textured  $\text{Al}_2\text{O}_3$ . *J Eur Ceram Soc*, 1995, **15**, 283–289.
5. Seabaugh, M. M., Kerscht, I. H. and Messing, G. L., Texture development by templated grain growth in liquid-phase sintered  $\alpha$ -alumina. *J Am Ceram Soc*, 1997, **80**, 1181–1188.
6. Suvaci, E. and Messing, G. L., Critical factors in the templated grain growth of textured reaction-bonded alumina. *J Am Ceram Soc*, 2000, **83**, 2041–2048.
7. Seabaugh, M. M., Messing, G. L. and Vaudin, M. D., Texture development and microstructure evolution in liquid-phase-sintered  $\alpha$ -alumina ceramics prepared by templated grain growth. *J Am Ceram Soc*, 2000, **83**, 3109–3116.
8. Wei, M., Zhi, D. and Brandon, D. G., Microstructure and texture evolution in gel-cast  $\alpha$ -alumina/alumina platelet ceramic composites. *Scripta Mater*, 2005, **53**, 1327–1332.
9. Ozer, I. O., Suvaci, E., Karademir, B., Missiaen, J. M., Carry, C. P. and Bouvard, D., Anisotropic sintering shrinkage in alumina ceramics containing oriented platelets. *J Am Ceram Soc*, 2006, **89**, 1972–1976.
10. Van der Biest, O. and Vandeperre, L. J., Electrophoretic deposition of materials. *Ann Rev Mater Sci*, 1999, **29**, 327–352.
11. Boccaccini, A. R., Roether, J. A., Thomas, B. J. C., Shaffer, M. S. P., Chavez, E., Stoll, E. et al., The electrophoretic deposition of inorganic nanoscaled materials. *J Ceram Soc Jpn*, 2006, **114**, 1–14.
12. Menon, M., Decourcelle, S., Ramousse, S. and Larsen, P. H., Stabilization of ethanol-based alumina suspensions. *J Am Ceram Soc*, 2006, **89**, 457–464.
13. Lotgering, F. K., Topotactical reactions with ferromagnetic oxides having hexagonal crystal structures. *J Inorg Nucl Chem*, 1959, **9**, 113–123.
14. Gönenli, I. E. and Messing, G. L., Texturing of mullite by templated grain growth with aluminum borate whiskers. *J Eur Ceram Soc*, 2001, **21**, 2495–2501.
15. Bunge, H. J., *Texture analysis in materials science: mathematical models*. Butterworths, London, 1982, pp. 119–152.
16. Belmonte, M., Moya, J. S. and Miranzo, P., Bimodal sintering of  $\text{Al}_2\text{O}_3/\text{Al}_2\text{O}_3$  platelet ceramic composites. *J Am Ceram Soc*, 1995, **78**, 1661–1667.
17. Suder, O. and Lange, F. F., Effect of inclusions on densification: I, microstructural development in an  $\text{Al}_2\text{O}_3$  matrix containing a high volume fraction of  $\text{ZrO}_2$  inclusions. *J Am Ceram Soc*, 1992, **75**, 519–524.
18. Eng, P. J., Trainor, T. P., Brown, G. E., Waychunas, G. A., Newville, M., Sutton, S. R. et al., Structure of the hydrated  $\alpha$ - $\text{Al}_2\text{O}_3$  (0001) surface. *Science*, 2000, **288**, 1029–1033.
19. Franks, G. V. and Gan, Y., Charging behavior at the alumina-water interface and implications for ceramic processing. *J Am Ceram Soc*, 2007, **90**, 3373–3388.
20. Hunter, R. J., *Foundations of colloid science*. Oxford University Press, New York, 1986, pp. 25–32.
21. Mody, N. A., Lomakin, O., Doggett, T. A., Diacovo, T. G. and King, M. R., Mechanics of transient platelet adhesion to von willebrand factor under flow. *Biophys J*, 2005, **88**, 1432–1443.
22. Harnau, L. and Dietrich, S., Fluids of platelike particles near a hard wall. *Phys Rev E*, 2002, **65**, 021505.
23. Dimasi, E., Fossum, J. O., Gog, T. and Venkataraman, C., Orientational of in gravity dispersed clay colloids: a synchrotron x-ray scattering study of Na fluorohectorite suspensions. *Phys Rev E*, 2001, **64**, 061704.
24. Van der Kooij, F. M. and Lekkerkerker, H. N. W., Formation of nematic liquid crystals in suspensions of hard colloidal platelets. *J Phys Chem B*, 1998, **102**, 7829–7832.